Supporting Information for

Mechanochemical Synthesis of Phase-Pure Zirconium Metal-Organic Cages

Loris Lombardo* [a,b], Ellan K. Berdichevsky[c], Farzaneh Fadaei-Tirani[d], Shin-Ichi Orimo[a,e], Andreas Züttel[b], Satoshi Horike*[f,g,h]

[a] *Institute for Materials Research, Tohoku University, Sendai, Miyagi 980-8577, Japan*

[b] *Institute of Chemical Sciences and Engineering, Basic Science Faculty, École polytechnique fédérale de Lausanne (EPFL) Valais/Wallis, Energypolis, Rue de l'Industrie 17, 1951 Sion, Switzerland*

[c] *Department of Synthetic Chemistry and Biological Chemistry, Graduate School of Engineering, Kyoto University, Katsura, Nishikyo-ku, Kyoto 615-8510, Japan*

[d] *Institut des Sciences et Ingénierie Chimiques, École Polytechnique Fédérale de Lausanne (EPFL), 1015 Lausanne, Switzerland.*

[e] *Institute for Materials Research and Advanced Institute for Materials Research (WPI-AIMR), Tohoku University, Sendai, Miyagi 980-8577, Japan*

[f] *Department of Chemistry, Graduate School of Science, Kyoto University, Kitashirakawa-Oiwakecho, Sakyo-ku, Kyoto 606-8502, Japan*

[g] *Institute for Integrated Cell-Material Sciences, Institute for Advanced Study, Kyoto University, Yoshida-Honmachi, Sakyo-ku, Kyoto 606-8501, Japan*

[h] *Department of Materials Science and Engineering, School of Molecular Science and Engineering, Vidyasirimedhi Institute of Science and Technology, Rayong 21210, Thailand*

Contents

Experimental Part

Zirconocene dichloride (Cp_2ZrCl_2, >97.0%, TCI), benzoic acid (Bz, ≥99.5%, Sigma-Aldrich), acetic acid (HOAc, glacial, Merck), terephthalic acid (BDC, 98%, Sigma-Aldrich), 2,6-naphthalenedicarboxylic acid (2,6-ndc, >98.0%, TCI), 2-aminoterephthalic acid (BDC-NH_2, 99%, Sigma-Aldrich), trimesic acid (BTC, 95%, Sigma-Aldrich), 1,3,5-tris(4-carboxyphenyl)benzene (BTB, ≥98%, Sigma-Aldrich), and 2,5-dihydroxyterephthalic acid (BDC-$(OH)_2$, 98%, Sigma-Aldrich) were used as received.

Synthesis of zirconium clusters

Synthesis of $[Zr_3(\mu_3\text{-}O)(\mu_2\text{-}OH)_3(Cp)_3(BA)_3]Cl$ (ZrCp-BA-cluster)

The preparation was carried out according to previous reports.[1,2] In short, Cp_2ZrCl_2 (2.4 mmol) was dissolved in dichloromethane (DCM, 35 mL). Benzoic acid (2.4 mmol) was dissolved in 10 mL H_2O with the addition of NaOH (1 mmol). The pH of the solution was adjusted to 6-7 with HCl. The benzoic acid solution was then added dropwise to the Cp_2ZrCl_2 solution under vigorous stirring. The reaction was stirred for 30 minutes at room temperature. Then, the mixture was left undisturbed for 24 hours to allow the phases to separate. The white precipitate was filtered and washed with fresh DCM. Finally, the powder was dried under vacuum at room temperature (yield: 74%).

Synthesis of $[Zr_3(\mu_3\text{-}O)(\mu_2\text{-}OH)_3(Cp)_3(OAc)_3]Cl$ (ZrCp-OAc-cluster)

The preparation was performed in accordance with a previously published report.[3] The method is identical to the preparation of ZrCp-BA-cluster, with acetic acid (2.4 mmol) used instead of benzoic acid. The pH of the HOAc solution was adjusted to 8-9. Typical yield: 60%.

Mechanochemical synthesis of zirconium metal-organic cages

The mechanochemical synthesis of cages was carried out using a planetary ball mill (Fritsch, Pulverisette 7). In a typical procedure, the Zr–SBU cluster (0.1 mmol) and the corresponding ligand (0.15 mmol for bidentate ligands; 0.1 mmol for tridentate ligands) were placed in a 12 mL zirconia milling jar along with 30 zirconium oxide balls (5 mm diameter). The ball-to-powder mass ratio was maintained at approximately 100:1. Milling was performed in the presence of DMF with a 15 min milling / 5 min rest cycle. The resulting material was collected and washed three times with 3 mL portions of DMF, followed by activation through solvent exchange with DCM for 3 days, refreshing the solvent every 12 h. The powders were activated at 60 °C under reduced pressure for 6 h before surface area measurement.

Synthesis of $[Zr_{12}(\mu_3\text{-}O)_4(\mu 2\text{-}OH)_{12}(Cp)_{12}(BDC\text{-}(OH)_2)_6]Cl_4$ (Zr-MOC-BDC-$(OH)_2$)

In a 4 mL glass vial, Cp_2ZrCl_2 (58.4 mg, 0.2 mmol) and BDC-$(OH)_2$ (19.8 mg, 0.1 mmol) were dissolved in DMA (3 mL). Then 250 µL of DI water was added. The solution was kept at room temperature for 2 days. The formed yellow cubic crystals were collected and soaked for 12 h in DMA and DCM, 3x each. The powder was activated at 60 °C under reduced pressure for 6 h before surface area measurement (Yield: ~30%).

Characterization

Zr-cluster and cages were characterized with a Fourier-transform infrared spectroscopy (FT-IR; Bruker Optics ALPHA, ATR accessory, Germany), Nuclear Magnetic Resonance spectroscopy (^{1}H NMR; Bruker 500 MHz AVIII, Germany), and powder X-ray Diffraction

(PXRD, Bruker D8 Advance, CuKα radiation). The cages' surface area was determined by N_2 isotherm measurements at 77 K (Microtrac Belsorb MAX II). Thermo-gravimetric analysis (TGA) was carried out under N_2 flow with a heating rate of 10 K min^{-1} (NETZSCH TG 209 F1 Libra). Electrospray Ionization Mass Spectrometry (ESI-MS) was measured by dissolving the cage in MeOH (Thermo Orbitrap Elite, nanochip-ESI, positive mode, LTQ-Orbitrap analyzer).

Single crystal measurement

A clear light-yellow cube-shaped crystal with dimensions 0.07 × 0.07 × 0.03 mm was mounted. Data were collected using a XtaLAB Synergy R, DW system, HyPix-Arc 150 diffractometer operating at T = 140.00(10) K.

Data were measured using *w* scans with Cu K_a radiation. The diffraction pattern was indexed, and the total number of runs and images was based on the strategy calculation from the program CrysAlis^{Pro} system (CCD 44.113a 64-bit (release 02-06-2025)).[4] The maximum resolution achieved was Q = 50.339°. The unit cell was refined using CrysAlis^{Pro} on 3652 reflections, 31% of the observed reflections.

Data reduction, scaling, and absorption corrections were performed using CrysAlis^{Pro}. The final completeness is 99.40 % out to 50.339° in Q. A Gaussian absorption correction was performed using CrysAlis^{Pro} 1.171.44.111a (Rigaku Oxford Diffraction, 2025) Numerical absorption correction based on Gaussian integration over a multifaceted crystal model. Empirical absorption correction using spherical harmonics as implemented in SCALE3 ABSPACK scaling algorithm. The absorption coefficient m of this material is 5.111 mm^{-1} at this wavelength (l = 1.54184Å), and the minimum and maximum transmissions are 0.767 and 0.927.

The structure was solved in the space group $Fm\bar{3}m$ (# 225) by ShelXT[5] using dual methods and by using Olex2 1.5 as the graphical interface.[6] It was refined by full matrix least squares minimisation on $|\boldsymbol{F}|^2$ using version 2019/3 of ShelXL 2019/3. All non-hydrogen atoms were refined anisotropically.

Most hydrogen atom positions were calculated geometrically and refined using the riding model, but the hydrogen atom on the bridging hydroxyl group (OH) was found in a difference map and refined freely.

A solvent mask was calculated and 7988 electrons were found in a volume of 28806$Å^3$ in 1 void per unit cell. This is consistent with the presence of 24 Dimethylacetamide solvent molecules per Asymmetric Unit which account for 9216 electrons per unit cell.

The value of Z' is 0.041667. The moiety formula is $C_{108}H_{84}O_{52}Zr_{12}$, 4($Cl_1$), 24[$C_4H_9NO$].

Results

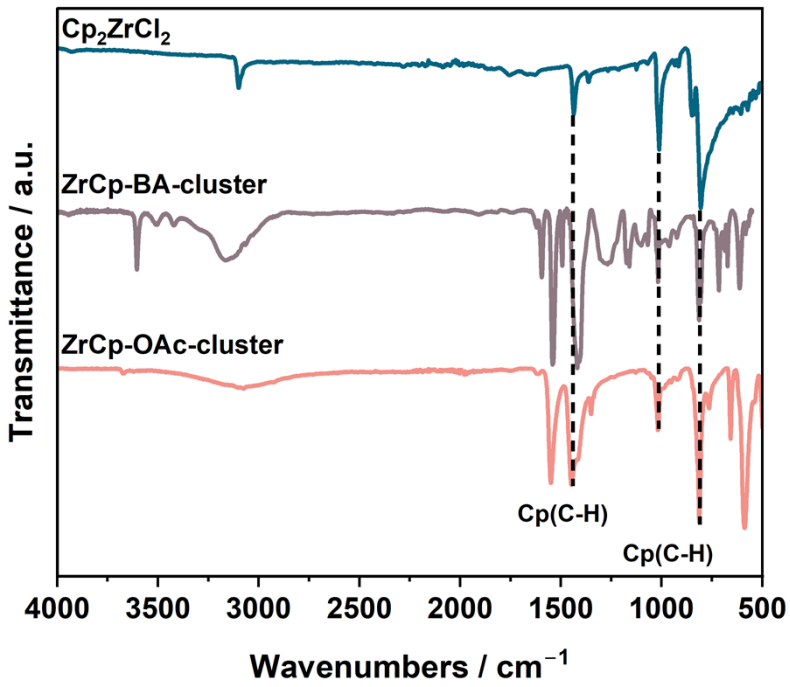

Figure S1: FT-IR spectra of Cp_2ZrCl_2 compared with the prepared ZrCp-BA-cluster and ZrCp-OAc-cluster.

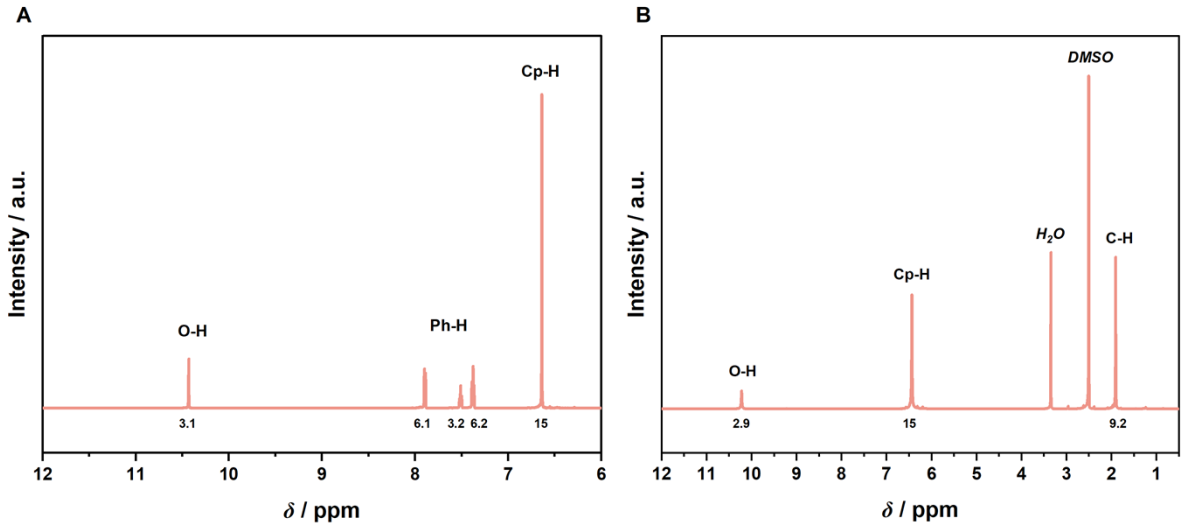

Figure S2: ^{1}H NMR spectra of **A** ZrCp-BA-cluster and **B** ZrCp-OAc-cluster (DMSO-d_6).

Table S1: Crystallographic data for ZrCp-BA-cluster.

Empirical formula	$C_{38}H_{41}ClO_{12}Zr_3$
Formula weight	998.82
Temperature / K	100
Crystal system	triclinic
Space group	$P\bar{1}$
a / Å	10.8213(2)
b / Å	11.2030(2)
c / Å	18.4411(4)
α / °	80.973(2)
β / °	83.6460(10)
γ / °	63.780(2)
Volume / Å^3	1978.60(8)

Z	2
ρ_{calc} / g cm^{-3}	1.676
μ / mm^{-1}	0.901
F(000)	1004.0
Crystal size / mm^3	0.2 × 0.1 × 0.05
Radiation	Mo Kα (λ = 0.71073)
2θ range for data collection / °	4.082 to 63.594
Index ranges	-15 ≤ h ≤ 15, -16 ≤ k ≤ 16, -18 ≤ l ≤ 26
Reflections collected	36914
Independent reflections	12068 [R_{int} = 0.0251, R_{sigma} = 0.0309]
Data/restraints/parameters	12068/0/503
Goodness-of-fit on F^2	1.057
Final R indexes [I>=2σ (I)]	R_1 = 0.0312, wR_2 = 0.0738
Final R indexes [all data]	R_1 = 0.0386, wR_2 = 0.0770
Largest diff. peak/hole / e Å^{-3}	0.78/-0.74

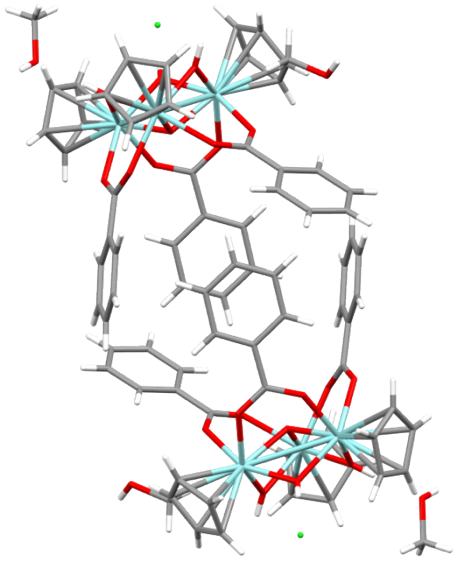

Figure S3: Structure of two ZrCp-BA-clusters from single crystal data. Grey: C, red: O, blue: Zr, white: H, green: Cl.

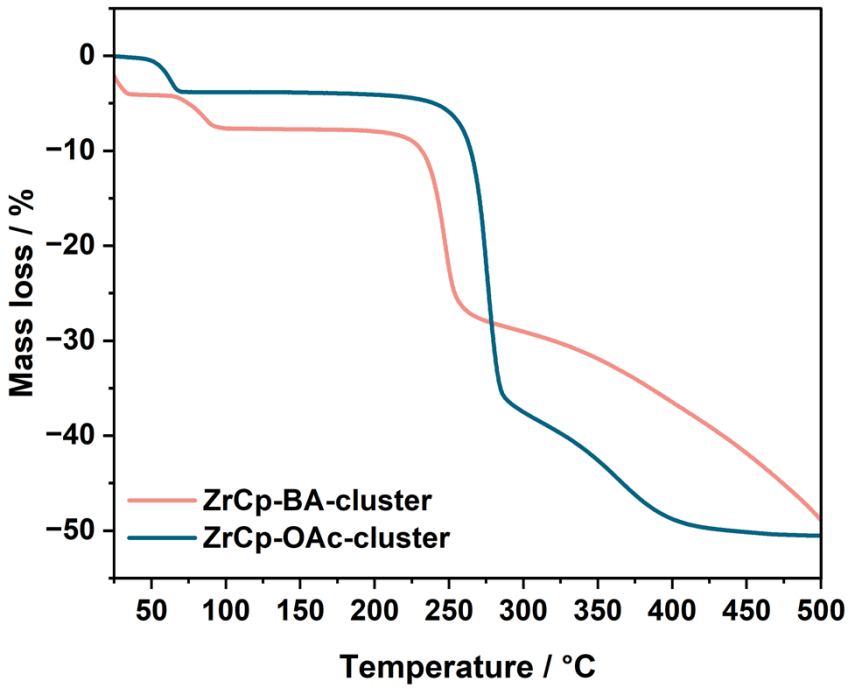

Figure S4: TGA curves of ZrCp-BA-cluster and ZrCp-OAc-cluster (N_2 flow, 10 K min^{-1}).

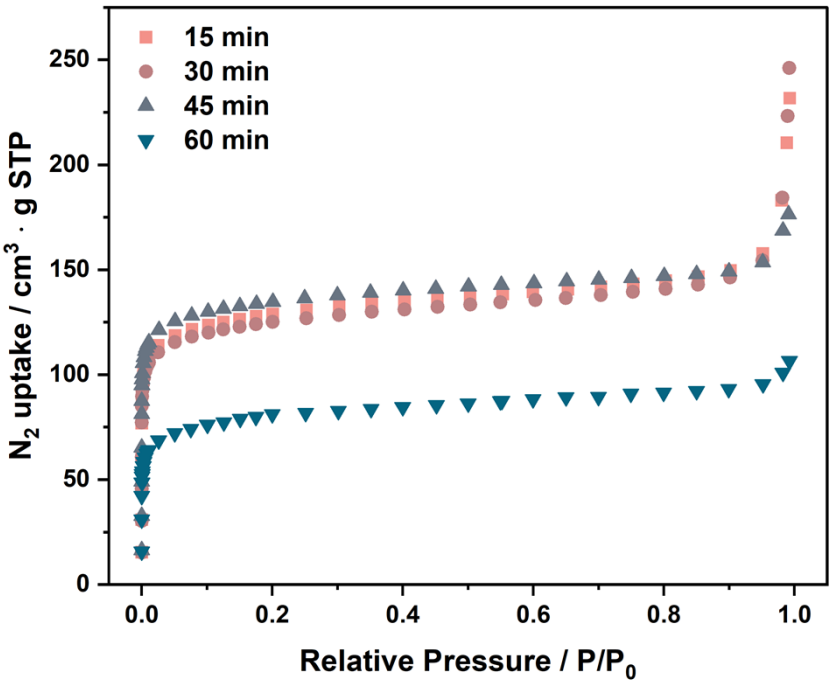

Figure S5: N_2 gas adsorption isotherms at 77 K for Zr-MOC-BDC with different milling times (DMF η=0.5 μL g^{-1}).

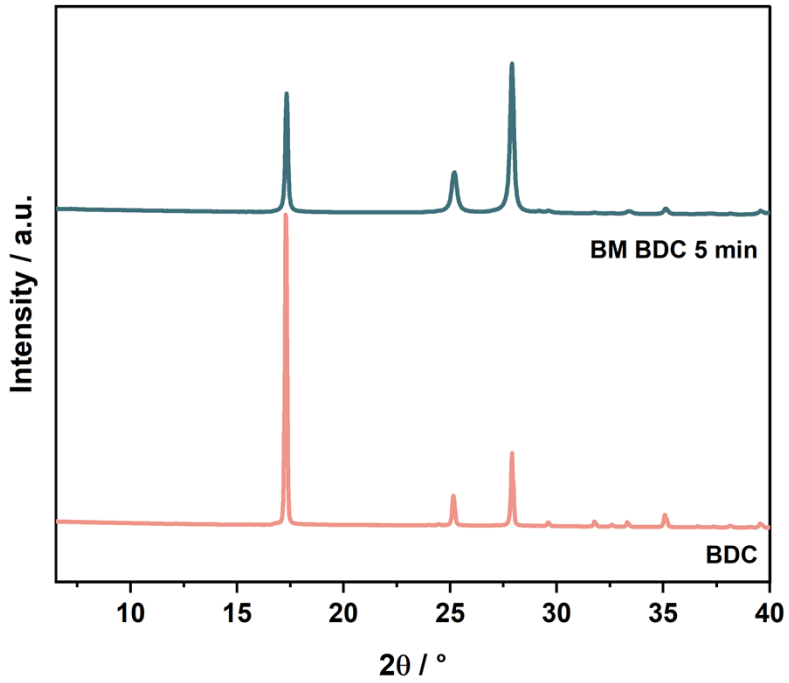

Figure S6: Normalized PXRD patterns of BDC before and after ball milling (BM) for 5 minutes at 500 rpm.

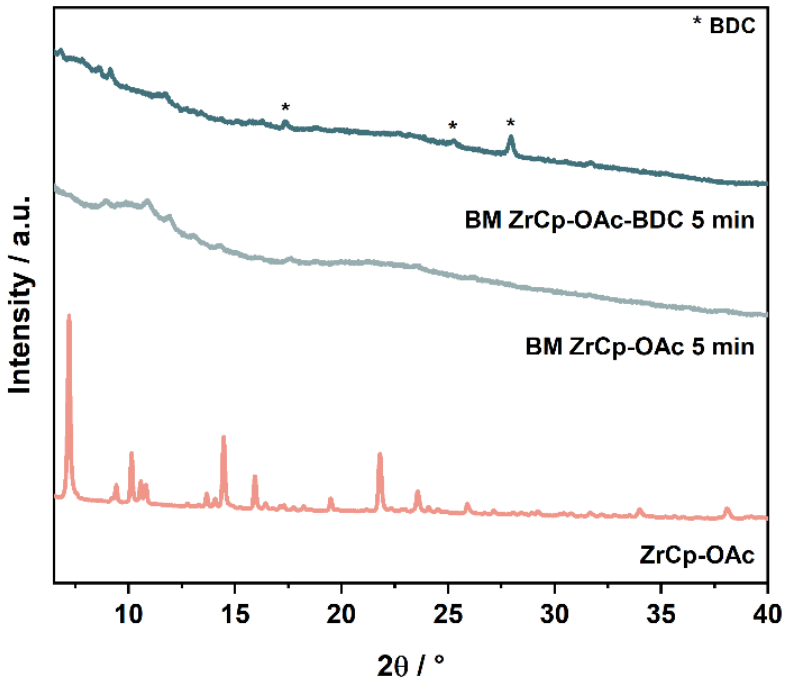

Figure S7: Normalized PXRD patterns of ZrCp-OAc before and after ball milling (BM) for 5 minutes at 500 rpm in the absence or presence of BDC.

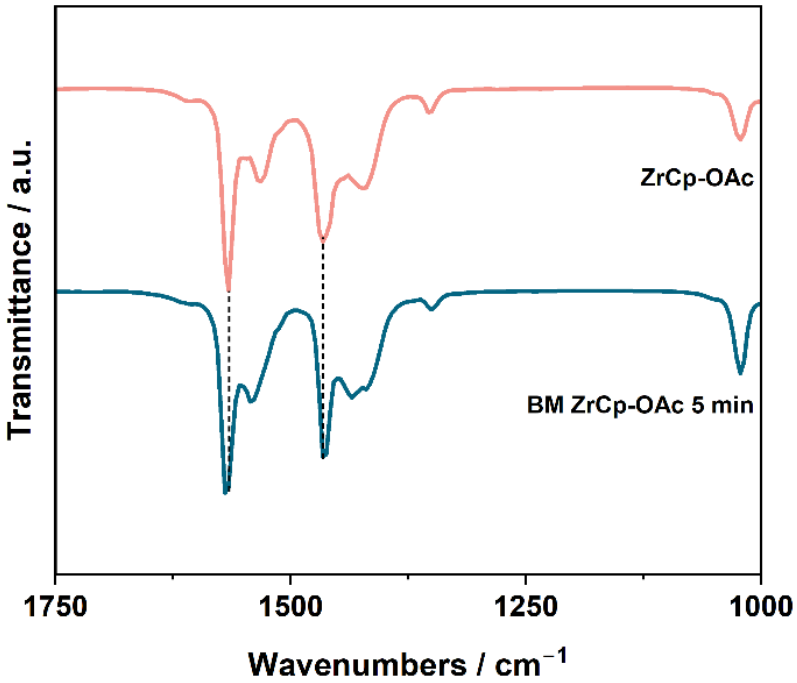

Figure S8: FT-IR spectra of ZrCp-OAc before and after ball milling (BM) for 5 minutes at 500 rpm.

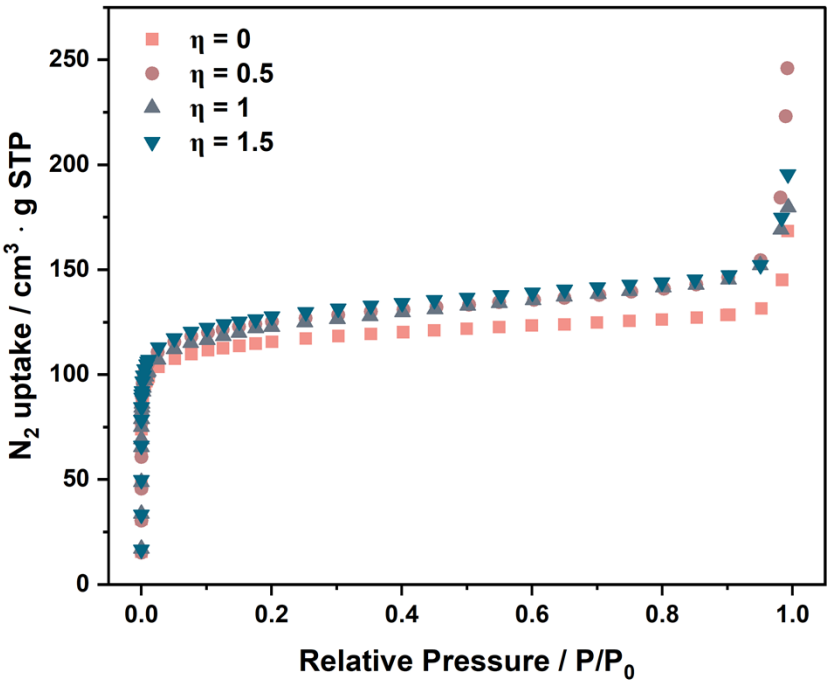

Figure S9: N_2 gas adsorption isotherms at 77 K for Zr-MOC-BDC with different DMF amounts (time: 30min).

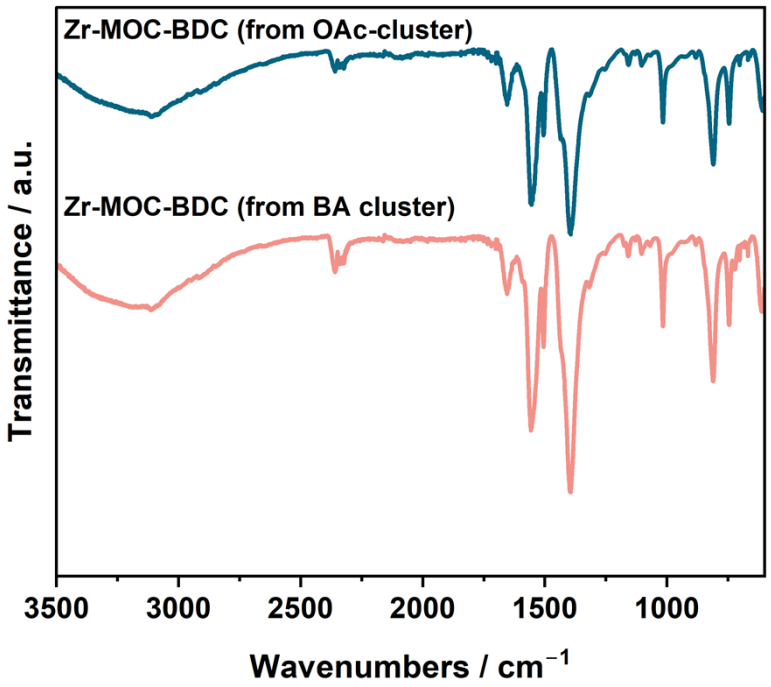

Figure S10: FT-IR spectra comparison of Zr-MOC-BDC prepared from ZrCp-OAc-cluster or ZrCp-BA-cluster.

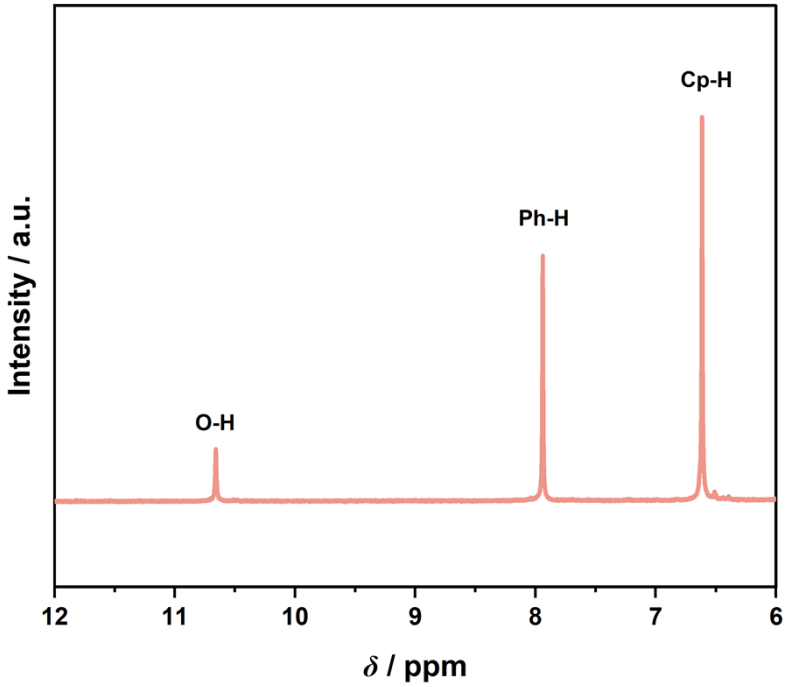

Figure S11: ^{1}H NMR in DMSO-d_6 spectrum of Zr-MOC-BDC prepared from ZrCp-OAc-cluster (DMF η=0.5 μL g^{-1}, 30 min).

Table S2: Time, energy, and solvent usage comparison for the synthesis of Zr-BDC for solvothermal and mechanochemical synthetic routes. A yield of 70% was assumed for both cases.

	Solvothermal	**Mechanochemical**
Time (h)	8	0.5
Energy consumption (kWh)	2.4-3.2[1]	0.35
Solvent usage (mL·g^{-1})	120	0.9 (100[2])

[1]Temperature: 60°C

[2]Including cluster synthesis

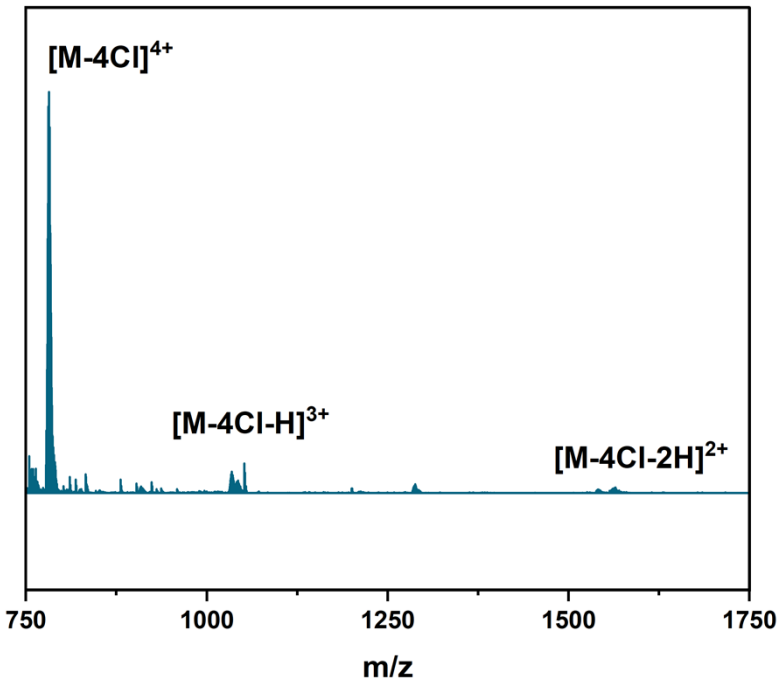

Figure S12: ESI-MS data of Zr-MOC-BDC in MeOH. The peaks at 781.5, 1043.1, and 1564.7 m/z are consistent with the 4+, 3+, and 2+ ions of the tetrahedron phase.

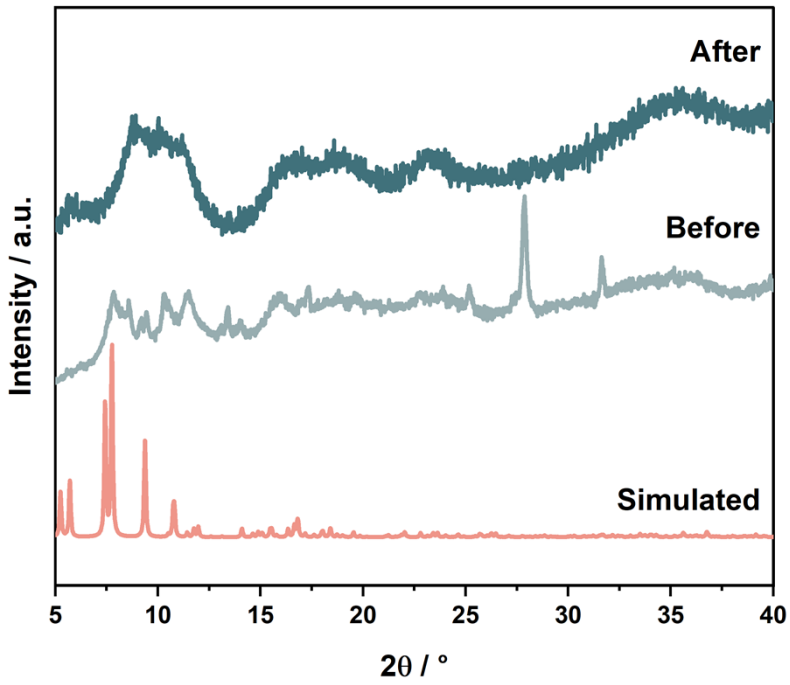

Figure S13: Normalized PXRD patterns of Zr-MOC-BDC before and after activation (DMF η=0.5 μL g^{-1}, 30 min) compared with the reported crystal structure. (CCDC: 950330).[7]

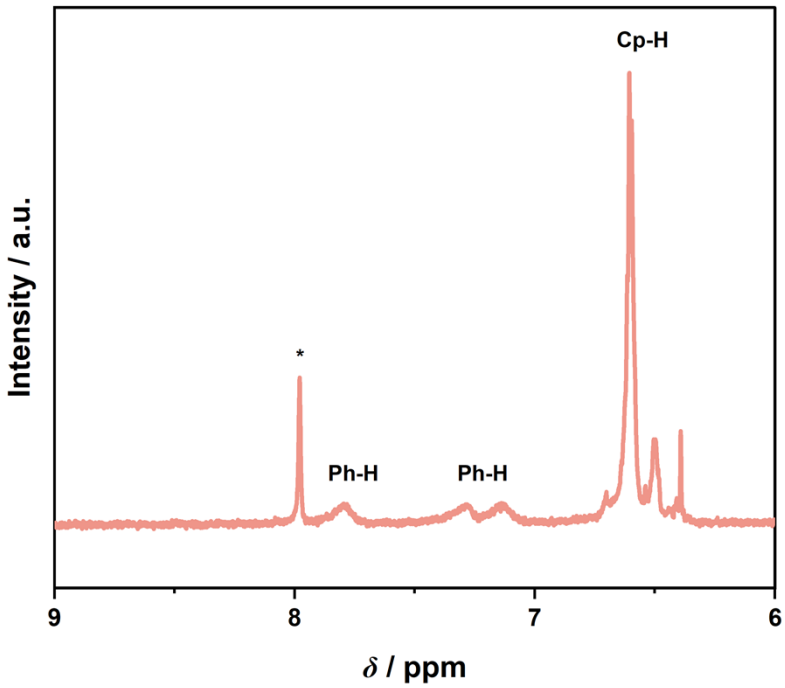

Figure S14: ^{1}H NMR spectrum of Zr-MOC-BDC-NH_2 in MeOD prepared from Zr-SBU-OAc (DMF η=0.5 µL g^{-1}, 30 min). * DMF trace.

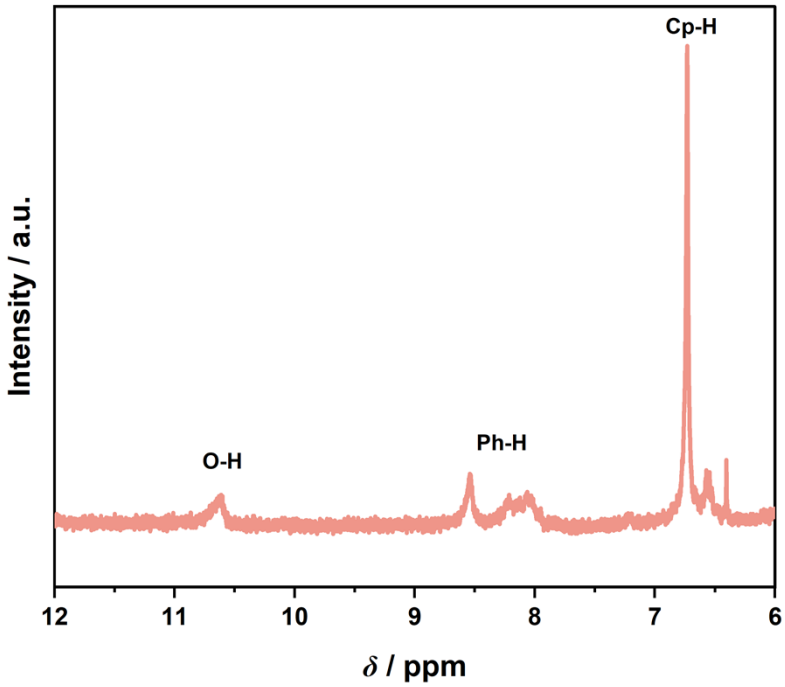

Figure S15: ^{1}H NMR spectrum of Zr-MOC -ndc in DMSO-d_6 prepared from Zr-SBU-OAc (DMF η=0.5 µL g^{-1}, 30 min).

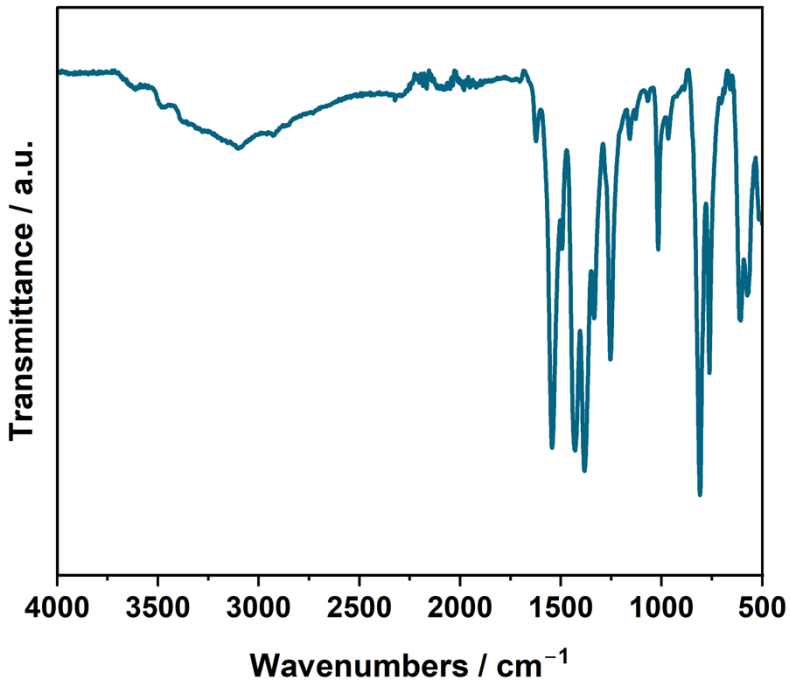

Figure S16: FT-IR spectra of Zr-MOC-BDC-NH_2.

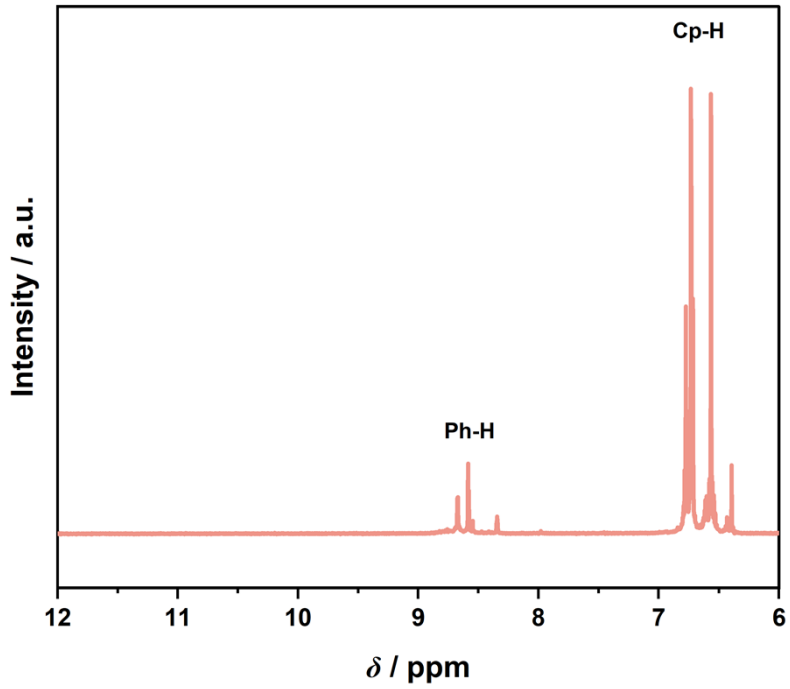

Figure S17: ^{1}H NMR spectrum of Zr-MOC-BTC in MeOD prepared from Zr-SBU-OAc (DMF η=0.5 µL g^{-1}, 30 min).

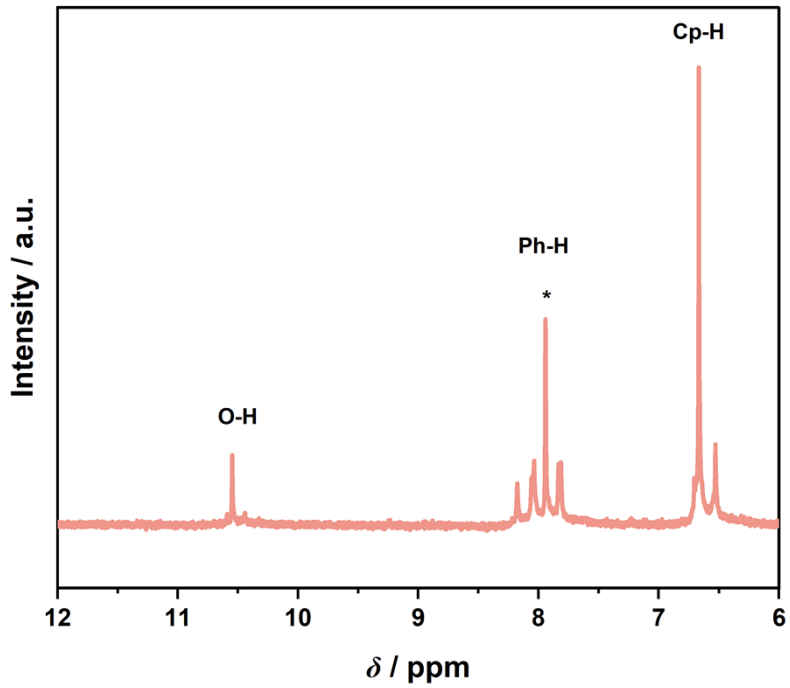

Figure S18: ^{1}H NMR spectrum of Zr-MOC-BTB in DMSO-d_6 prepared from Zr-SBU-OAc (DMF η=0.5 μL g^{-1}, 30 min). * DMF trace.

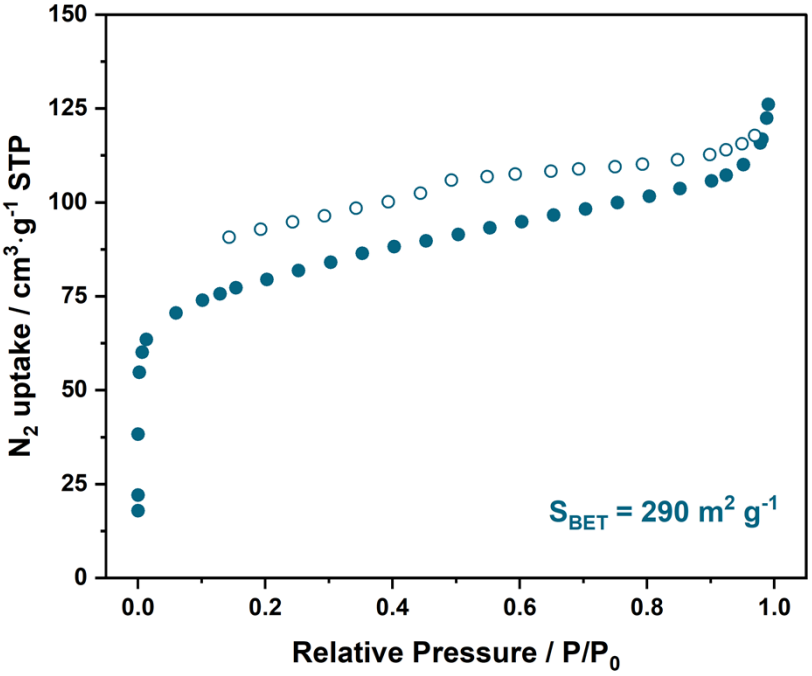

Figure S19: N_2 gas adsorption (fill) and desorption (hollow) isotherm of Zr-MOC-BDC-NH_2 at 77 K.

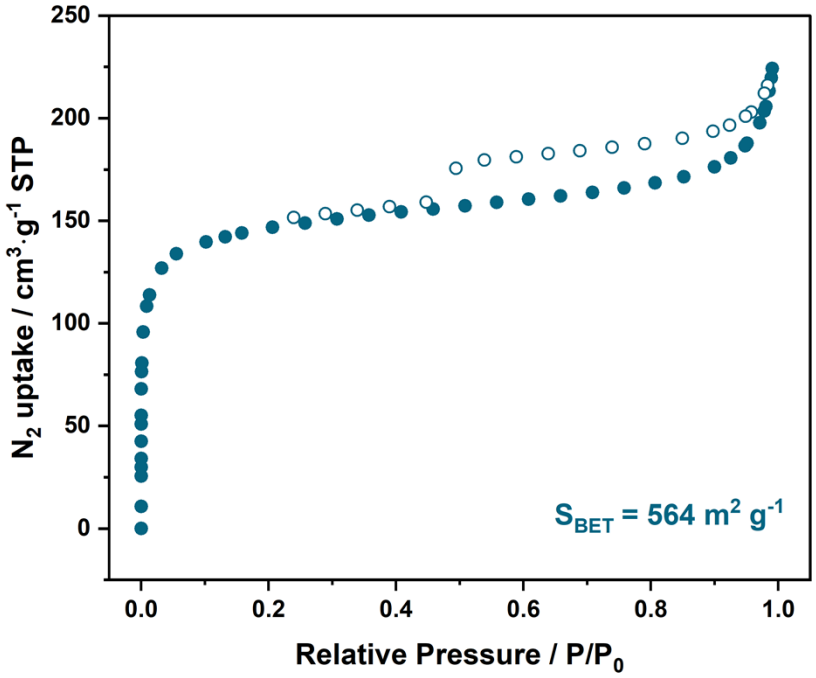

Figure S20: N_2 gas adsorption (fill) and desorption (hollow) isotherm of Zr-MOC-ndc at 77 K.

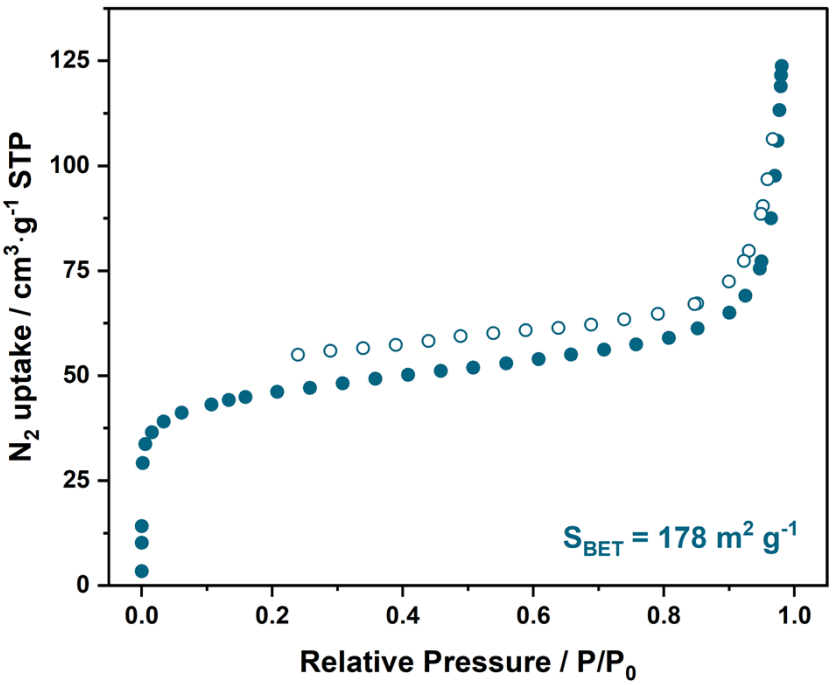

Figure S21: N_2 gas adsorption (fill) and desorption (hollow) isotherm of Zr-MOC-BTC at 77 K.

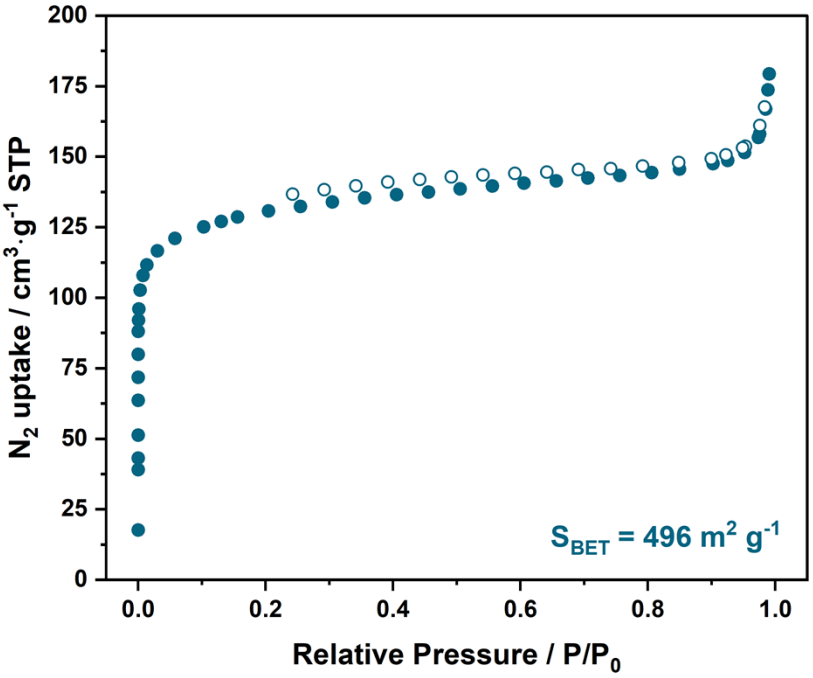

Figure S22: N_2 gas adsorption (fill) and desorption (hollow) isotherm of Zr-MOC-BTB at 77 K.

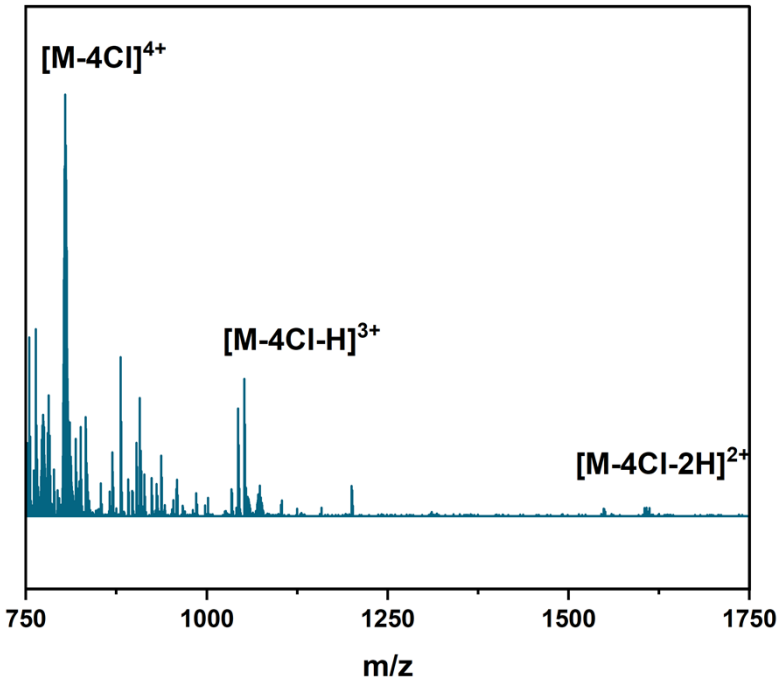

Figure S23: ESI-MS data of Zr-MOC-BDC-NH_2 in MeOH. The peaks at 804.4, 1073.2, and 1607.7 m/z are consistent with the 4+, 3+, and 2+ ions of the tetrahedron phase.

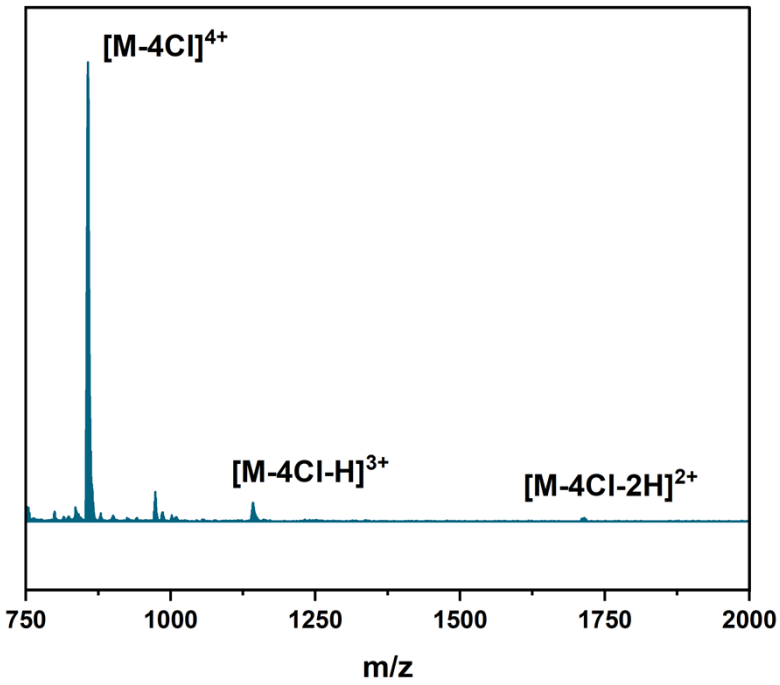

Figure S24: ESI-MS data of Zr-MOC-ndc in MeOH. The peaks at 856.9, 1141.2, and 1711.8 m/z are consistent with the 4+, 3+, and 2+ ions of the tetrahedron phase.

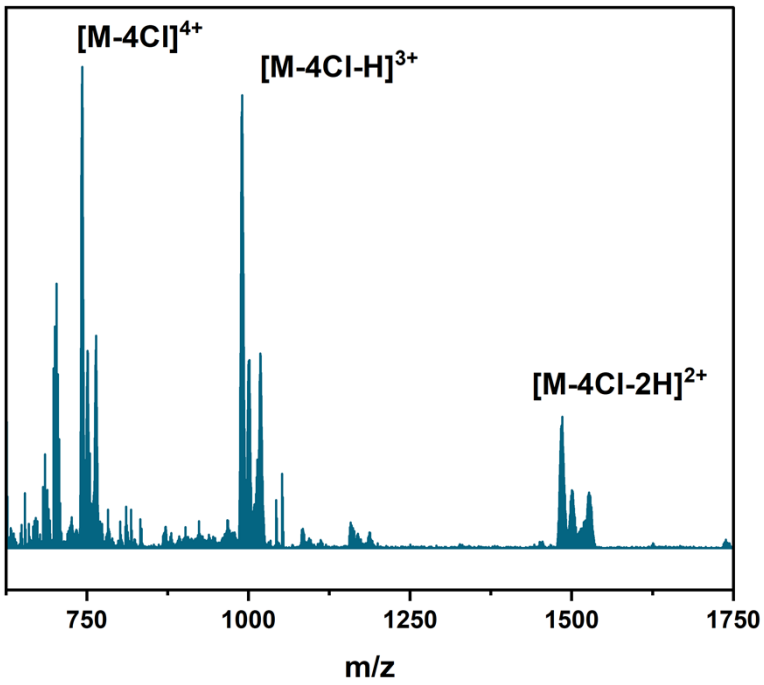

Figure S25: ESI-MS data of Zr-MOC-BTC in MeOH. The peaks at 743.1, 990.4, and 1484.7 m/z are consistent with the 4+, 3+, and 2+ ions of the tetrahedron phase. Other signals observed at 751.1, 761.3, 764.3, 1001.4, 1013.8, 1018.4, 1500.2, 1521.2 and 1527.1 are attributed to Zr-MOC-BTC with DMF, DCM, or other molecules trapped inside.

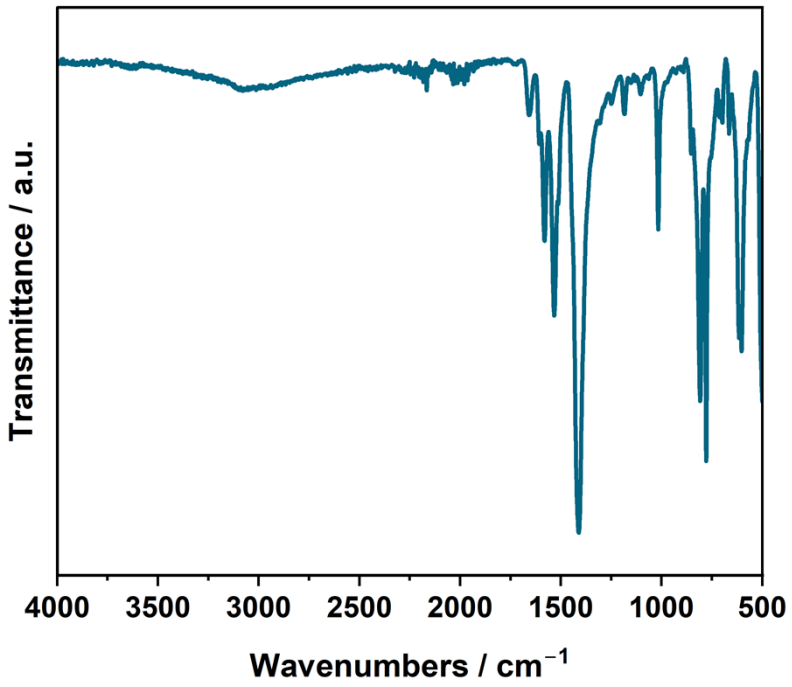

Figure S26: FT-IR spectra of Zr-MOC-BTB.

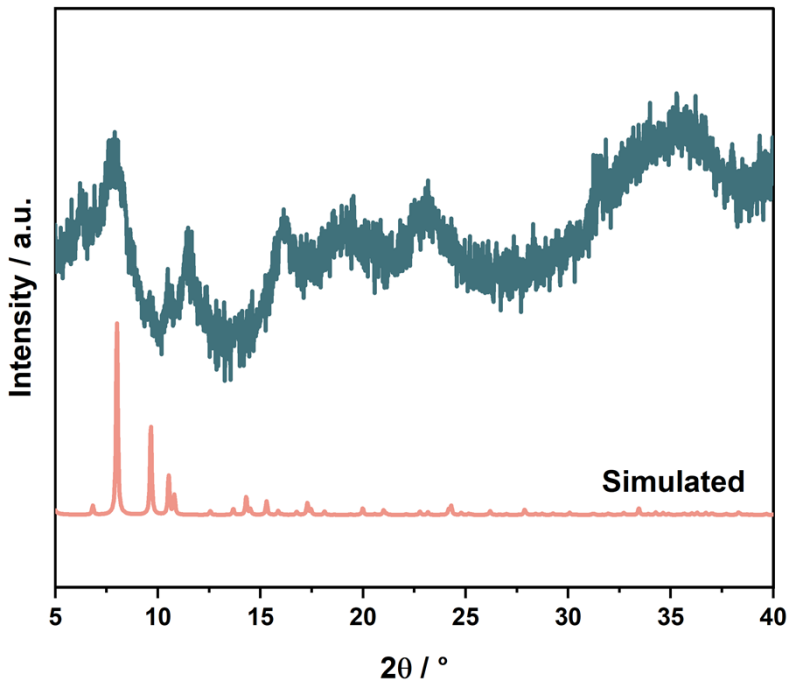

Figure S27: PXRD patterns of Zr-MOC-BDC-NH_2 before activation (DMF η=0.5 μL g^{-1}, 30 min) compared with the reported crystal structure. (CCDC: 2109985).[8]

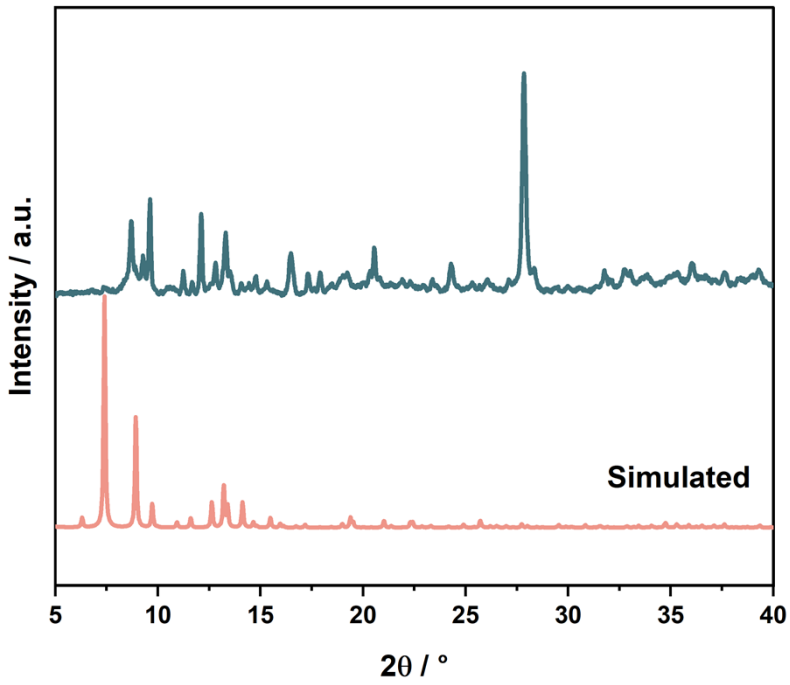

Figure S28: PXRD patterns of Zr-MOC-ndc before activation (DMF η=0.5 μL g^{-1}, 30 min) compared with the reported crystal structure. (CCDC: 1955203).[9]

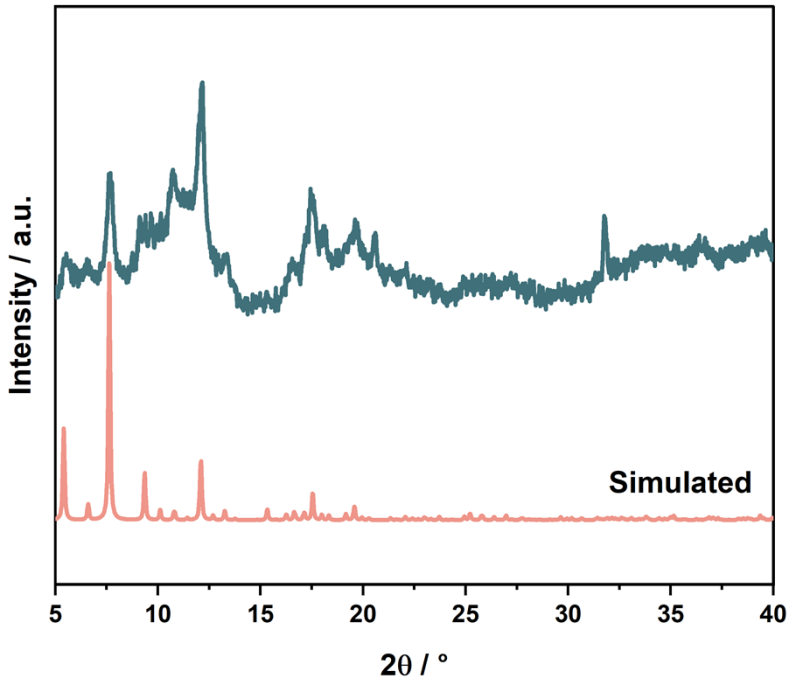

Figure S29: PXRD patterns of Zr-MOC-BTC before activation (DMF η=0.5 μL g^{-1}, 30 min) compared with the reported crystal structure. (CCDC: 950331).[7]

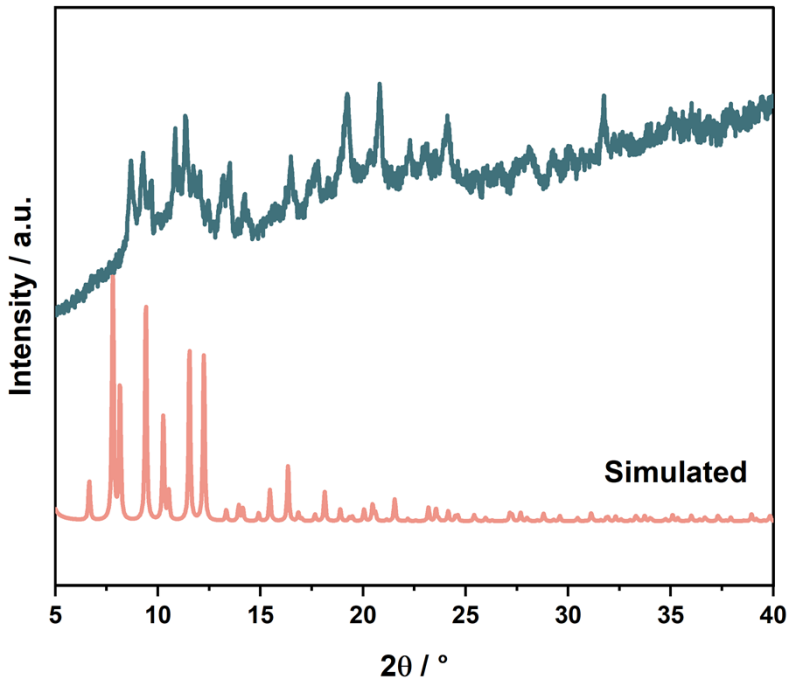

Figure S30: PXRD patterns of Zr-MOC-BTB before activation (DMF η=0.5 μL g^{-1}, 30 min) compared with the reported crystal structure. (CCDC: 950333).[7]

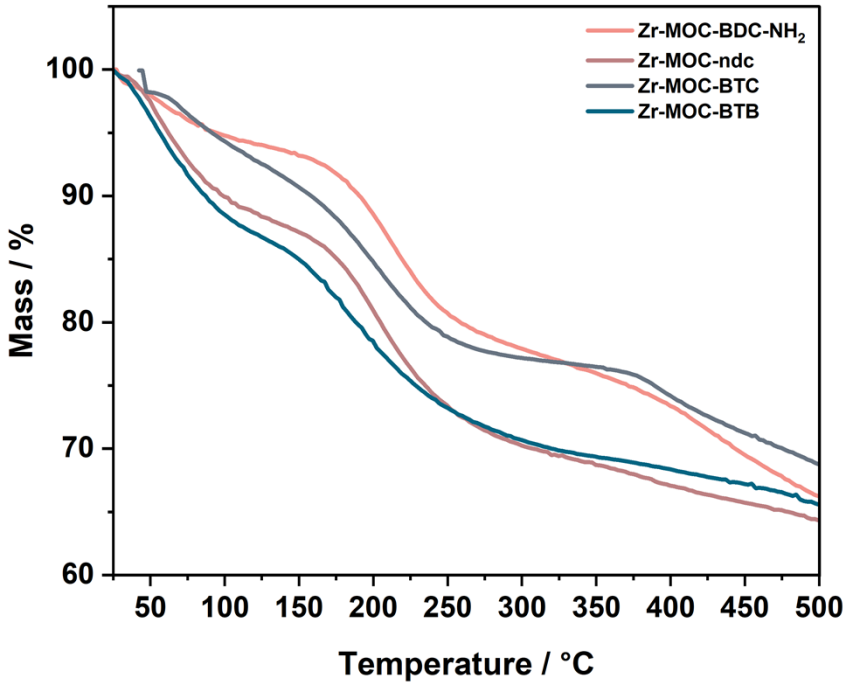

Figure S31: TGA curves of the mechanochemically prepared Zr-cages.

Table S3: Crystallographic data for **Zr-MOC-BDC-(OH)$_2$**.

Formula	$C_{204}H_{300}Cl_4N_{24}O_{76}Zr_{12}$
$D_{calc.}$/ g cm^{-3}	1.454
μ/mm^{-1}	5.111
Formula Weight	5541.10
Colour	clear light yellow
Shape	cube-shaped
Size/mm	0.07×0.07×0.03
T/K	140.00(10)
Crystal System	cubic
Space Group	$Fm\bar{3}m$
a / Å	36.6442(6)
b / Å	36.6442(6)
c / Å	36.6442(6)
α / °	90
β / °	90
γ / °	90
V / Å^3	49206(2)
Z	8
Z'	0.041667
Wavelength / Å	1.54184
Radiation type	Cu K$_a$
Θ_{min} / °	2.088

Θ_{max} / °	50.339
Index range h	-16 ≤ h ≤ 36
Index range k	-36 ≤ k ≤ 25
Index range l	-33 ≤ l ≤ 27
Measured Refl's.	11717
Indep't Refl's	1332
Refl's I≥2*s*(I)	1079
R_{int}	0.0167
Parameters	86
Restraints	119
Largest Peak / eÅ^3	0.729
Deepest Hole / eÅ^3	-0.405
GooF	1.119
R_1 (I≥2*s*(I) / all)	0.0747 / 0.0815
wR_2 (I≥2*s*(I) / all)	0.2435 / 0.2535
CCDC number	2498546

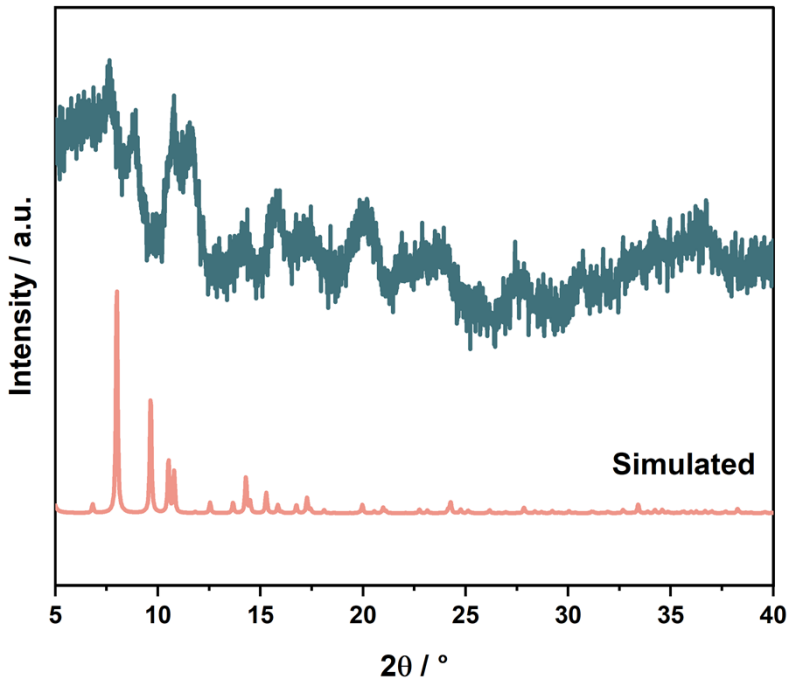

Figure S32: PXRD patterns of Zr-MOC-BDC-$(OH)_2$ before activation (DMF η=0.5 µL g^{-1}, 30 min) compared with the simulated crystal structure.

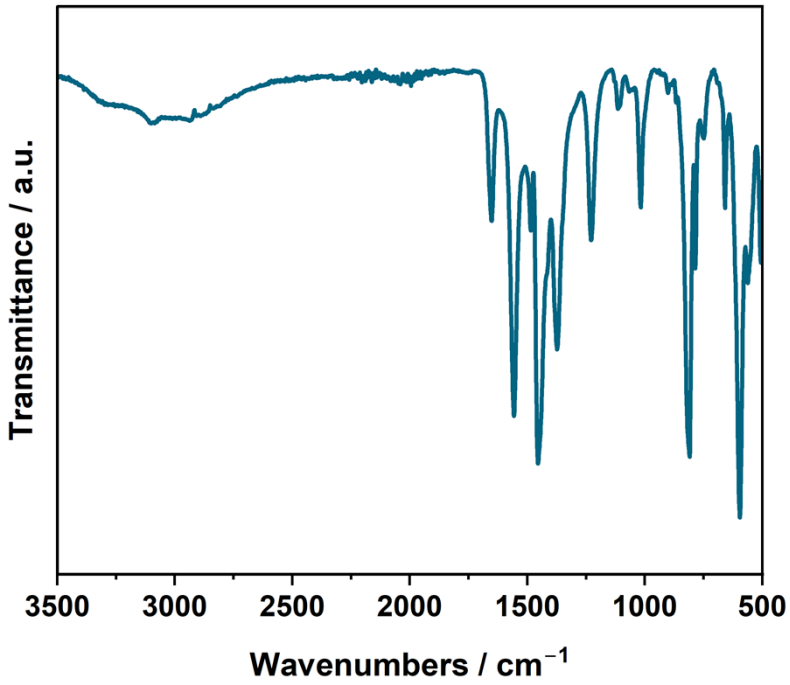

Figure S33: FT-IR spectra of D Zr-MOC-BDC-$(OH)_2$.

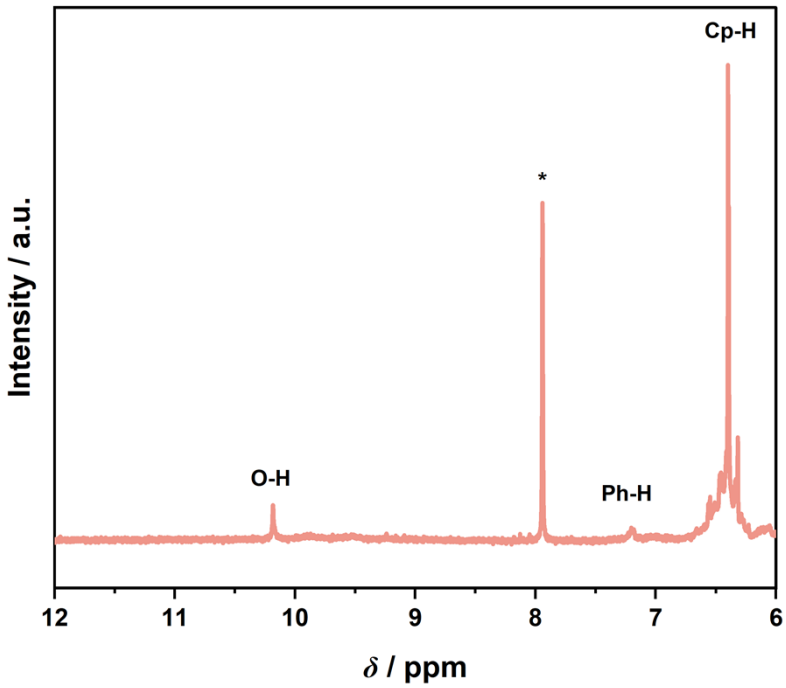

Figure S34: ^{1}H NMR spectrum of Zr-MOC-BDC-$(OH)_2$ in DMSO-d_6 prepared from Zr-SBU-OAc (DMF η=0.5 μL g^{-1}, 30 min). * DMF trace.

References

(1) Iden, H.; Bi, W.; Morin, J.-F.; Fontaine, F.-G. Zirconium(IV) Metallocavitands As Blue-Emitting Materials. *Inorg. Chem.* **2014**, *53* (6), 2883–2891. https://doi.org/10.1021/ic402602d.
(2) Sullivan, M. G.; Welgama, H. K.; Crawley, M. R.; Friedman, A. E.; Cook, T. R. Phase-Pure Zirconium Metal–Organic Polyhedra Enabled by a Ligand Substitution Strategy. *Chem. Mater.* **2024**, *36* (1), 567–574. https://doi.org/10.1021/acs.chemmater.3c02775.
(3) Skalla, R. X.; Montone, C. M.; Pink, M.; Walters, O. K.; Bloch, E. D. Role of Solvent Decomposition in the Synthesis and Composition of Porous Zirconium-Based Coordination Cages. *Inorg. Chem.* **2025**. https://doi.org/10.1021/acs.inorgchem.4c04982.
(4) Sheldrick, G. M. SHELXT – Integrated Space-Group and Crystal-Structure Determination. *Acta Crystallogr. Sect. Found. Adv.* **2015**, *71* (1), 3–8. https://doi.org/10.1107/S2053273314026370.
(5) Sheldrick, G. M. Crystal Structure Refinement with SHELXL. *Acta Crystallogr. Sect. C Struct. Chem.* **2015**, *71* (1), 3–8. https://doi.org/10.1107/S2053229614024218.
(6) Dolomanov, O. V.; Bourhis, L. J.; Gildea, R. J.; Howard, J. a. K.; Puschmann, H. OLEX2: A Complete Structure Solution, Refinement and Analysis Program. *J. Appl. Crystallogr.* **2009**, *42* (2), 339–341. https://doi.org/10.1107/S0021889808042726.
(7) Liu, G.; Ju, Z.; Yuan, D.; Hong, M. In Situ Construction of a Coordination Zirconocene Tetrahedron. *Inorg. Chem.* **2013**, *52* (24), 13815–13817. https://doi.org/10.1021/ic402428m.
(8) Qin, L.-Z.; Xiong, X.-H.; Wang, S.-H.; Meng, L.-L.; Yan, T.-A.; Chen, J.; Zhu, N.-X.; Liu, D.-H.; Wei, Z.-W. A Series of Functionalized Zirconium Metal–Organic Cages for Efficient CO2/N2 Separation. *Inorg. Chem.* **2021**, *60* (23), 17440–17444. https://doi.org/10.1021/acs.inorgchem.1c02948.
(9) Gosselin, A. J.; Decker, G. E.; McNichols, B. W.; Baumann, J. E.; Yap, G. P. A.; Sellinger, A.; Bloch, E. D. Ligand-Based Phase Control in Porous Zirconium Coordination Cages. *Chem. Mater.* **2020**, *32* (13), 5872–5878. https://doi.org/10.1021/acs.chemmater.0c01965.